AIP Advances

Magnetic coupling of divalent metal centers in postsynthetic metal exchanged bimetallic DUT-49 MOFs by EPR spectroscopy

Cite as: AIP Advances **13**, 015019 (2023); https://doi.org/10.1063/9.0000532
Submitted: 03 October 2022 • Accepted: 03 November 2022 • Published Online: 19 January 2023

Kavipriya Thangavel, Matthias Mendt, Bikash Garai, et al.

Magnetic coupling of divalent metal centers in postsynthetic metal exchanged bimetallic DUT-49 MOFs by EPR spectroscopy

Cite as: AIP Advances 13, 015019 (2023); doi: 10.1063/9.0000532
Submitted: 3 October 2022 • Accepted: 3 November 2022 •
Published Online: 19 January 2023

View Online Export Citation CrossMark

Kavipriya Thangavel,[1,2,a)] Matthias Mendt,[1] Bikash Garai,[3] Andrea Folli,[2] Volodymyr Bon,[3] Damien M. Murphy,[2] Stefan Kaskel,[3] and Andreas Pöppl[1,b)]

AFFILIATIONS

[1] Felix Bloch Institute for Solid State Physics, University of Leipzig, Linnestrasse. 5, 04103 Leipzig, Germany
[2] School of Chemistry, Cardiff University, Park Place, Cardiff CF10 3AT, United Kingdom
[3] Department of Inorganic Chemistry, Technische Universität Dresden, Bergstraße 66, 01069 Dresden, Germany

Note: This paper was presented at the 67th Annual Conference on Magnetism and Magnetic Materials.
[a)]**Author to whom correspondence should be addressed:** ThangavelK@cardiff.ac.uk
[b)]**E-mail:** poeppl@physik.uni-leipzig.de

ABSTRACT

EPR measurements at X- (9.5 GHz), Q- (34 GHz) and W-band (94 GHz) on paddlewheel (PW) type post-synthetic metal exchanged DUT-49(M,M): M- Zn, Mn, Cu MOFs are here reported (DUT–Dresden University of Technology). Temperature-dependent X-band measurements are recorded from T = 7 K to T = 170 K on monometallic DUT-49(Cu), DUT-49(Mn), and bimetallic DUT-49($Cu_{0.7}Zn_{0.3}$), DUT-49($Cu_{0.5}Mn_{0.5}$) MOFs. In the case of the Cu^{II} - Cu^{II} dimers in DUT-49(Cu), an isotropic exchange coupling of the metal ions ($2J = -240(11)\ cm^{-1}$) determined from the EPR intensity of the $S = 1$ spin state of the Cu^{II}–Cu^{II} dimers using the Bleaney Blowers equation. The sign of the found isotropic exchange coupling constant confirms an antiferromagnetic coupling between the cupric ions. Also, the Mn^{II} ions in the paddle wheels of DUT-49(Mn) are antiferromagnetically coupled. However, at low temperatures, EPR measurements reveal the presence of Cu^{II} and Mn^{II} monomers in DUT-49(Cu) and DUT-49(Mn), respectively, either associated with extra framework sites or defective paddle wheels. Otherwise, EPR signals observed for bimetallic DUT-49($Cu_{0.7}Zn_{0.3}$) and DUT-49($Cu_{0.5}Mn_{0.5}$) MOFs reveal the formation of mixed ion Cu^{II}–Zn^{II} and Cu^{II}–Mn^{II} paddle wheels with S_{CuZn} =1/2 and S_{CuMn} = 2 spin states, respectively.

I. INTRODUCTION

Owing to the potential applications such as gas storage and separation, catalysis, heat storage, liquid purification, supercapacitors, drug delivery and dielectrics, metal-organic frameworks (MOFs) have attracted much attention in the present decade.[1,2] Among MOFs, DUT-49 (DUT–Dresden University of Technology) has gained much attention due to its breathing effect on gas adsorption[3] and negative gas adsorption[4] (NGA). Recently, NuMOF technologies first commercialized a MOF product for toxic gas storage.[5] Furthermore, understanding the magnetic properties of MOFs can help drive innovation in the field of molecular magnetism.[6] Electron paramagnetic resonance (EPR) spectroscopy is a unique tool to investigate the local geometric and electronic structure as well as the magnetic properties of paramagnetic ions in MOF materials.[1,3,7] EPR has been employed on MOF materials to understand catalytic properties,[1] intra- and intermolecular interactions,[8] structural changes upon gas[3] and liquid adsorption, magnetic properties,[7,8] post-ion exchange modification,[9] and photochromism due to UV laser irradiation.[10] Moreover, a series of paddle wheel (PW) based M^{II}–M^{II} dimers were investigated by EPR in DUT-49(Cu) upon *in situ* n-butane and Et_2O adsorption,[3] DUT-8($Ni_{1-x}Mn_x$) upon CO_2 adsorption,[11] DUT-8(Ni) upon N_2 and NO adsorption,[12,13] post ion exchange modified $Fe_xCu_{(3-x)}(BTC)_2$[9] and parent $Cu_3(BTC)_2$[7] upon nitroxide radical adsorption,[14] and bimetallic $Zn_xCu_{(3-x)}(BTC)_2$[15] upon olefin adsorption.[16]

In this work, we investigated the magnetic coupling of mono- and binuclear Cu^{II}, Zn^{II}, and Mn^{II} dimer centers in the PW units of the DUT-49(M,M) MOFs (Figure S1). The temperature-dependent EPR data at the X- and Q-band frequencies evidence the excited state antiferromagnetic exchange interaction of the metal dimers upon increasing temperature.

II. EXPERIMENTAL TECHNIQUES

See supplementary material Sec. S2 for the synthesis[17] and EPR instrumentation part.

III. RESULTS AND DISCUSSION

Temperature-dependent CW-X band EPR measurements were performed in the range 7 K < T <170 K for four MOFs, illustrated in Figs. 1(a)–1(d). No dominant EPR signals of Co(II) could be detected after the post-synthetic metal ion exchange procedure in the four studied samples. The species M (~260 mT < $\boldsymbol{B}$ < ~360 mT) in Figs. 1(a) and 1(b) indicates the Cu^{II} monomer having a $3d^9$ ground state with an electron spin S = 1/2 interacting with the nuclear spin I^{Cu} = 3/2 of the two copper isotopes $^{63,65}Cu$. The spin Hamiltonian for the Cu^{II} monomer M species can be written as

$$\hat{H} = \beta_e \boldsymbol{B}\hat{g}\boldsymbol{S} + \boldsymbol{S}\hat{A}\boldsymbol{I}^{\boldsymbol{Cu}} \quad (1)$$

Where the first term corresponds to the Zeeman splitting between electron spin S = 1/2 of Cu^{II} ion and applied magnetic field $\boldsymbol{B}$ (β_e – Bohr magneton, $\hat{g}$ – g tensor), and the second term represents the Cu^{II} electron-nuclear hyperfine (hf) interaction ($\hat{A}$ – hyperfine splitting (hfs) tensor and $\boldsymbol{I}^{\boldsymbol{Cu}}$ = 3/2 nuclear spin of $^{63,65}Cu$). The simulated spin Hamiltonian parameters of Cu^{II} monomer [Fig. 2(a)] for the monometallic DUT-49(Cu) are g_{xx} = 2.052(3), g_{yy} = 2.060(2), g_{zz} = 2.335(4), $A_{xx,yy}$ = 30(5) MHz, A_{zz} = 545(8) MHz which could be assigned to the defective Cu-Cu paddlewheel units or extra framework cupric ions.[7,9]

The spectral features illustrated in Fig. 1(b) for bimetallic DUT-49($Cu_{0.7}Zn_{0.3}$) are similar to the monometallic DUT-49(Cu) MOF [Fig. 1(a)]. However, in bimetallic DUT-49($Cu_{0.7}Zn_{0.3}$), 30% Zn^{II} incorporation on the Cu^{II} sites yields more Cu^{II} monomer species in comparison with DUT-49(Cu) and shows the intense signal of Cu^{II} monomer species till 170 K at ~260 mT < $\boldsymbol{B}$ < ~360 mT

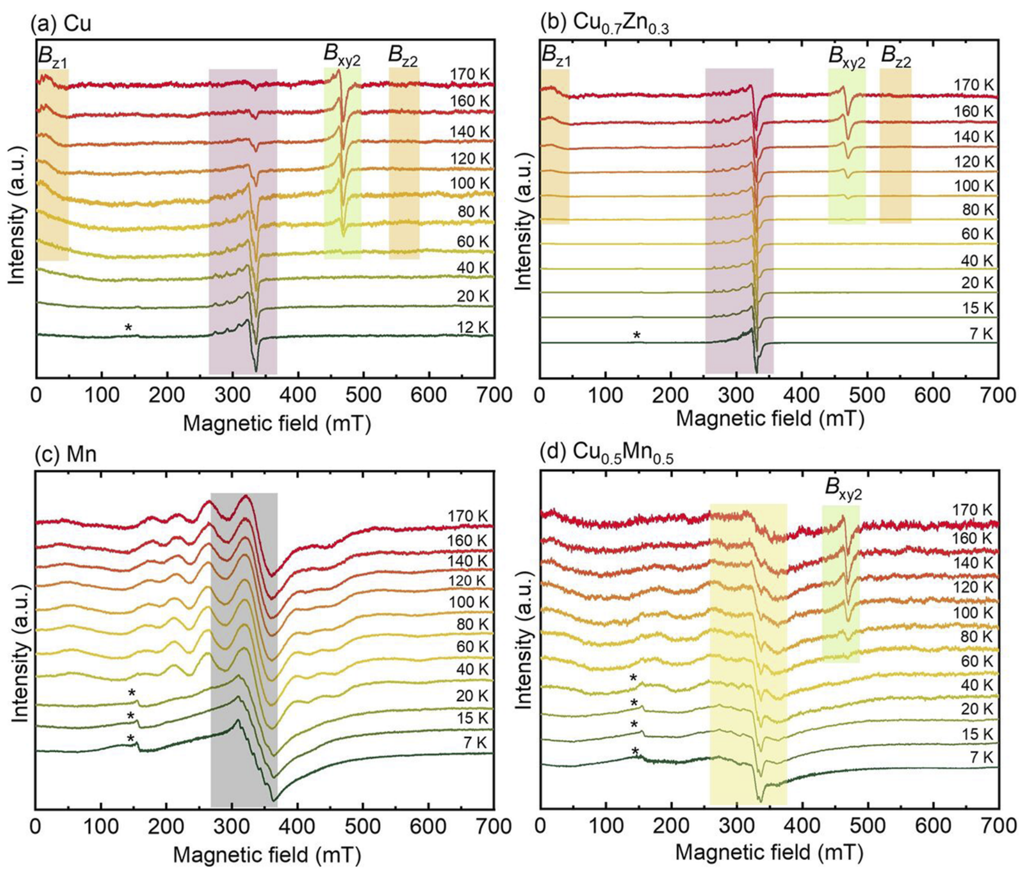

FIG. 1. Temperature-dependent X-band EPR experiments from T = 7 K to T = 170 K for (a) DUT-49(Cu), (b) DUT-49($Cu_{0.7}Zn_{0.3}$), (c) DUT-49(Mn), (d) DUT-49($Cu_{0.5}Mn_{0.5}$) (∗ a weak signal at ~150 mT indicates the minor Co^{II} impurity species, violet bar in (a) and (b) - S = 1/2 Cu^{II} monomer, gray bar in (c) - a mixture of S =1/2 Cu^{II} and S = 5/2 Mn^{II} monomers, and yellow bar in (d) - S = 5/2 Mn^{II} monomer).

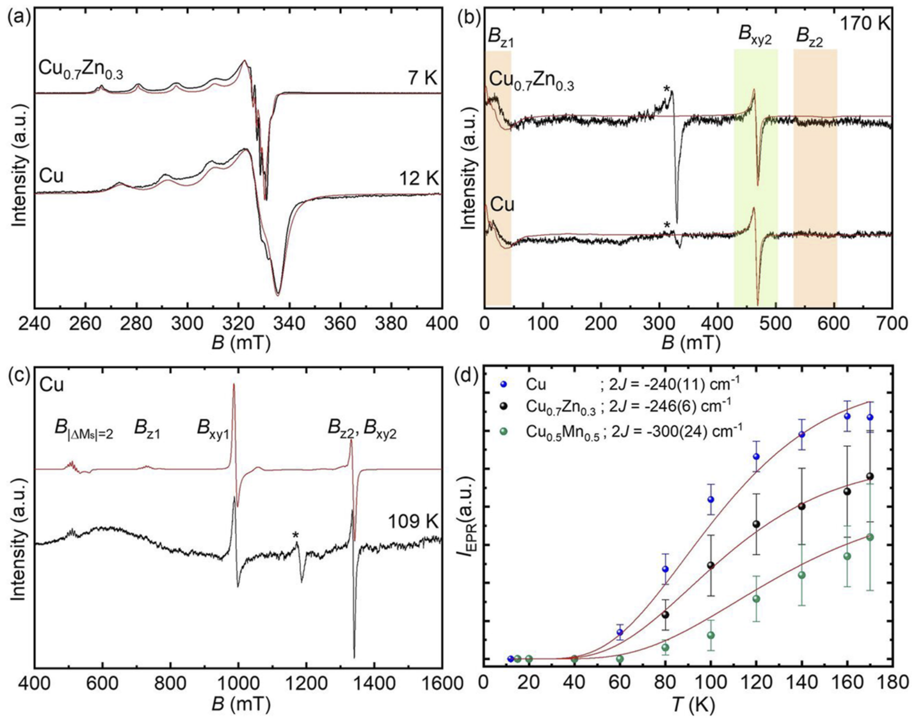

FIG. 2. Experimental (black) and simulated (red) spectra of (a) the $S = 1/2$ spin state of the Cu^{II} monomer, (b) the $S = 1$ spin state of the Cu^{II}–Cu^{II} dimer of DUT-49(Cu) and DUT-49($Cu_{0.7}Zn_{0.3}$) at X-band frequency, (c) the $S = 1$ spin state of the Cu^{II}–Cu^{II} dimer of DUT-49(Cu) at Q-band frequency (for the spin Hamiltonian parameters, see the text, * signals in (b) and (c) indicate $S = 1/2$ Cu^{II} monomer) and (d) The intensity extracted from the temperature-dependent X-band EPR data of DUT-49(M, M) fitted using Bleaney Bowers susceptibility equations for the coupled $S = 1/2$ dimer species. (Blue points - DUT-49(Cu), black points - DUT-49($Cu_{0.7}Zn_{0.3}$), green points - DUT-49($Cu_{0.5}Mn_{0.5}$), and red line – Bleaney Bowers susceptibility fit).

magnetic field range. This confirms the presence of Cu^{II}–Zn^{II} PW combination within the framework. The simulated spin Hamiltonian parameters of Cu^{II} monomer [Fig. 2(a)] for the bimetallic DUT-49($Cu_{0.7}Zn_{0.3}$) are $g_{xx} = 2.048(5)$, $g_{yy} = 2.073(4)$, $g_{zz} = 2.333(4)$, $A_{xx} = 26(3)$ MHz, $A_{yy} = 40(5)$ MHz, $A_{zz} = 470(8)$ and the values are consistent with the PW based Cu^{II} monomer species for the bimetallic $Zn_{0.03}Cu_{2.97}(BTC)_2$ MOF[15] with secondary species B (17%) where $g_{xx} = 2.0284(4)$, $g_{yy} = 2.0602(5)$, $g_{zz} = 2.3350(4)$, $A_{xx,yy} = 25(3)$ MHz and $A_{zz} = 479(7)$ MHz.

Moreover, the experimental results of DUT-49(Cu) clearly show the formation of Cu^{II}–Cu^{II} dimer above 60 K, where the two cupric ions with their $S = 1/2$ spin states couple to a total $S = 1$ state in the PW unit. Likewise, DUT-49($Cu_{0.7}Zn_{0.3}$) and DUT-49($Cu_{0.5}Mn_{0.5}$) indicate the Cu^{II}–Cu^{II} dimer formation above 80 K. The Spin Hamiltonian parameters of the S =1 spin state of the Cu^{II}–Cu^{II} dimer were evaluated using the spin Hamiltonian

$$\hat{H} = \beta_e \boldsymbol{B}\hat{g}\boldsymbol{S} + DS_z^2 + E\left(S_x^2 + S_y^2\right) + \boldsymbol{S}\hat{A}\boldsymbol{I}^{\boldsymbol{Cu}} \tag{2}$$

Where D and E are the axial and rhombic zero-field splitting (zfs) parameters. For the DUT-49(Cu) and DUT-49($Cu_{0.7}Zn_{0.3}$) MOFs, parameters D = 9990(45) MHz with a strain of $\Delta D = 450$ MHz, $E = 0$, $g_{xx,yy} = 2.065(8)$, $g_{zz} = 2.355(6)$, $A_{xx,yy} = 10(6)$ MHz and $A_{zz} = 220(9)$ MHz were obtained from spectral simulations [Figs. 2(b) and 3(c)]. The zfs spectral features are labelled according to Wassermann *et al.*,[18] where B_{z1} and B_{z2} represent the parallel, and B_{xy1} (out of the X-band magnetic field range due to large zfs) and B_{xy2} represent the perpendicular zfs transitions of the Cu^{II}–Cu^{II} dimer. However, all spectral transitions of the $S = 1$ species belonging to the Cu^{II}–Cu^{II} dimer can be seen in the Q-band spectrum[Fig. 2(c)]. Weak signals (∗) at ~150 mT in Fig. 1 are tentatively assigned to high spin Co^{II} impurities (g = ~5.2–4.2) from the parent sample or defects.[12] The total spin states of Cu^{II}–Cu^{II}, Cu^{II}–Zn^{II}, Cu^{II}–Mn^{II}, and Mn^{II}–Mn^{II} metal dimers in the PW units at a temperature of 7 K (LS–low spin) and 160 K (HS–high spin) are mentioned in Table S1 (supplementary material).

The Cu^{II}–Cu^{II} dimers in the PW units are well separated by the long linker (H_4BBCDC), which prevents the inter dimer exchange interactions. Moreover, an EPR signal intensity of the $S = 1$ spin state of these magnetically coupled Cu^{II}–Cu^{II} dimers in the PW units, which is proportional to the magnetic susceptibility, was extracted from temperature-dependent X-band EPR data for all MOFs [Fig. 2(d)]. The isotropic coupling constant of the Cu^{II}–Cu^{II} dimer can be estimated using the Bleaney-Bowers susceptibility equation of exchange coupled identical dimer species with $S_1 = 1/2$ and $S_2 = 1/2$

$$I_{EPR} \propto \frac{1}{k_B T\left(3 + \exp\left(-\frac{2J}{k_B T}\right)\right)} \tag{3}$$

Here I_{EPR} is the EPR intensity extracted from the double integration of B_{xy2} and B_{z2} parts of the $S = 1$ signal, k_B is the Boltzmann's constant, and $2J$ is the isotropic coupling constant. The $2J$ - value is found to be $-240(11)$ cm^{-1}, $-246(6)$ cm^{-1} and $-300(24)$ cm^{-1} for DUT-49(Cu), DUT-49($Cu_{0.7}Zn_{0.3}$) and DUT-49($Cu_{0.5}Mn_{0.5}$) MOFs, respectively [Fig. 2(d)]. The sign of the $2J$ - value indicates the excited state of antiferromagnetically coupled dimers, where the $S = 1$ triplet state is the thermally populated excited state, and

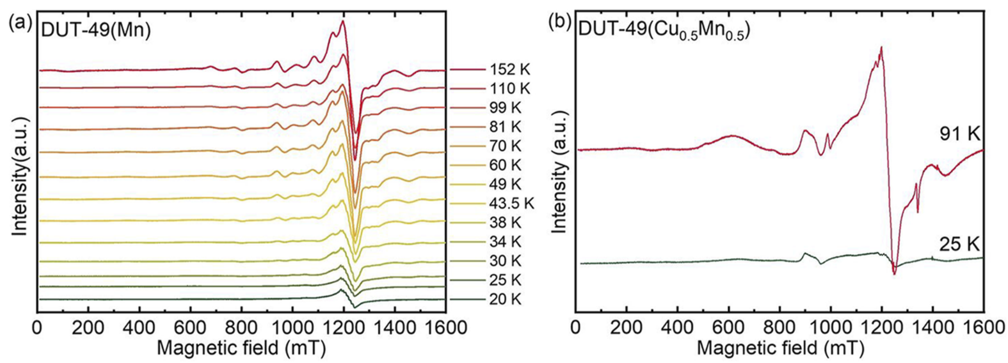

FIG. 3. Temperature-dependent Q-band EPR spectra of (a) DUT-49(Mn) and (b) DUT-49($Cu_{0.5}Mn_{0.5}$) MOFs.

the S = 0 singlet state corresponds to the ground state. Such an antiferromagnetic (AFM) exchange coupling is the characteristic behavior of Cu^{II}–Cu^{II} PW species.[3,7,19]

Figure 1(c) shows the temperature-dependent X-band EPR spectra of DUT-49(Mn). The low-temperature spectrum at T = 7 K shows a signal at g = 2.007 with a resolved hfs into six lines [Fig. S2(a)]. The g-value and the hfs sextet are characteristics of isolated Mn^{II} ion[20] with an S = 5/2 high spin state and a hyperfine interaction (hfi) with the ^{55}Mn nucleus having I^{Mn} = 5/2 characterised by an isotropic hyperfine coupling constant of A_{iso} = 240 MHz. The spectrum exhibits only the central $M_S = 1/2 \leftrightarrow -1/2$ spin transitions, whereas the outer $M_S = \pm 1/2 \leftrightarrow \pm 3/2$ and $M_S = \pm 3/2 \leftrightarrow \pm 5/2$ transitions are not resolved presumably because of large D strain effects. For spectra recorded at T > 30 K [Figs. 1(c) and S2(a)], a new multiline spectrum emerges, covering a broad field range of ~150 mT < $\boldsymbol{B}$ < ~550 mT at X-band frequencies. The intensity of this spectrum increase with rising temperatures. A comparable behavior is observed in the temperature-dependent Q-band spectra of DUT-49(Mn) [Fig. 3(a)]. Based on the multiline characteristic and temperature dependence, we may assign this spectrum to AFM-coupled Mn^{II}–Mn^{II} dimers. In this case of AFM coupled Mn^{II} dimers, we expect total spin states S = 0, 1, 2, 3, 4, and 5 (S = 0 singlet ground state), which is increasingly populated with rising temperatures. However, the poor resolution of the X- and Q- band spectra prevented a determination of the Spin Hamiltonian parameters of the Mn^{II}–Mn^{II} dimers here by simulation or fitting procedures. CW W- band spectra did not provide a better resolution and suffered from poor signal-to-noise ratios.

Meanwhile, the low-temperature X- band [Figs. 1(d) and S2(b)] and Q- band [Fig. 3(b)] EPR spectra of DUT-49($Cu_{0.5}Mn_{0.5}$) show the coexistence of Cu^{II} and Mn^{II} monomer species with the emergence of Cu^{II}–Cu^{II} dimer as well upon increasing temperature above 80 K. Some characteristic spectral features of the Mn^{II}–Mn^{II} dimers at about ~1450 mT, ~1200 mT, and ~900 mT are likewise distinguishable at Q-band whereas the X band spectra suffer here from low signal to noise ratios and poor resolution except for the Cu^{II}–Cu^{II} dimer spectrum. An additional low field signal at ~700 mT in the Q-band spectrum indicates the existence of further magnetic species in DUT-49($Cu_{0.5}Mn_{0.5}$), which we tendentially assign to an AFM coupled Cu^{II}–Mn^{II} dimer with possible total spin states S = 2 and S = 3.

IV. CONCLUSION

EPR spectroscopy revealed for both transition metal dimers, Cu^{II}–Cu^{II} and Mn^{II}–Mn^{II}, in the paddle wheel units of MOFs DUT-49(Cu) and DUT-49(Mn) an antiferromagnetic coupling. Besides these metal dimers in the regular paddle wheel units, monomeric paramagnetic Cu^{II} and Mn^{II} species are observed, which most likely indicates the presence of defective paddle wheels with a missing metal ion. In the case of the mixed metal ion MOF DUT-49($Cu_{0.7}Zn_{0.3}$), the formation of binuclear paramagnetic Cu^{II}–Zn^{II} dimers besides the antiferromagnetic coupled Cu^{II}–Cu^{II} dimers in the paddlewheel units could be confirmed. More complicated spectra have been obtained for MOF DUT-49($Cu_{0.5}Mn_{0.5}$) that allowed for the unambiguous identification of Cu^{II}–Cu^{II} dimers and further indicated the presence of Mn^{II}–Mn^{II} dimers and AFM coupled Cu^{II}–Mn^{II} dimers. Our results confirm the feasibility of the post-synthetic metal ion exchange of Co^{II} in the DUT-49 framework by other divalent transition metal ions such as Cu^{II}, Zn^{II}, and Mn^{II} through the magnetic coupling of the divalent metal centers.

SUPPLEMENTARY MATERIAL

See supplementary material for the structure of the paddle wheel unit and the comparison of CW X-band EPR experiments at low and 160 K temperatures.

ACKNOWLEDGMENTS

The authors acknowledge the financial support of the Deutsche Foschungsgemeinschaft (DFG) within the research unit FOR2433 (MOF switches). Authors K.T, D.M.M and A.P thank the European Union's H2020 MSCA project PARACAT Grant agreement No: 813209.

AUTHOR DECLARATIONS

Conflict of Interest

The authors have no conflicts to disclose.

Author Contributions

Kavipriya Thangavel: Formal analysis (lead); Investigation (lead); Writing – original draft (lead). **Matthias Mendt**: Formal analysis (equal); Investigation (equal); Software (equal). **Bikash Garai**: Methodology (equal); Resources (equal). **Andrea Folli**: Formal analysis (equal); Writing – review & editing (equal). **Volodymyr Bon**: Methodology (equal); Resources (equal). **Damien M. Murphy**: Formal analysis (equal); Supervision (equal). **Stefan Kaskel**: Methodology (equal); Resources (equal).

DATA AVAILABILITY

The data that support the findings of this study are available within the article and its supplementary material.

REFERENCES

[1]M. Bracci, P. C. Bruzzese, A. Famulari, D. Fioco, A. Guidetti, Y.-K. Liao, L. Podvorica, S. F. Rezayi, I. Serra, K. Thangavel, and D. M. Murphy, in *Electron Paramagnetic Resonance*, edited by B. E. Bode, V. Chechik, and D. M. Murphy (Royal Society of Chemistry, Cambridge, 2021), Vol. 27, p. 1.

[2]S. Mukherjee, S. Sharma, and S. K. Ghosh, APL Materials **7**, 050701 (2019).

[3]D. M. Polyukhov, S. Krause, V. Bon, A. S. Poryvaev, S. Kaskel, and M. V. Fedin, The Journal of Physical Chemistry Letters **11**, 5856 (2020).

[4]J. D. Evans, L. Bocquet, and F.-X. Coudert, Chem **1**, 873 (2016).

[5]NuMat Technologies, https://www.numat.tech/.

[6]H. S. C. Hamilton, W. M. Farmer, S. F. Skinner, and L. W. ter Haar, AIP Advances **8**, 055802 (2018).

[7]A. Pöppl, S. Kunz, D. Himsl, and M. Hartmann, J. Phys. Chem. C **112**, 2678 (2008).

[8]EPR and SQUID interrogations of Cr (III) trimer complexes in the MIL-101 (Cr) and bimetallic MIL-100 (Al/Cr) MOFs, 2022.

[9]J. Bitzer, S. Otterbach, K. Thangavel, A. Kultaeva, R. Schmid, A. Pöppl, and W. Kleist, Chemistry (Weinheim an der Bergstrasse, Germany) **26**, 5667 (2020).

[10]J. Cornelio, S. J. Lee, T.-Y. Zhou, A. Alkaş, K. Thangavel, A. Pöppl, and S. G. Telfer, Chemistry of Materials **34**, 8437 (2022).

[11]M. Mendt, M. Maliuta, S. Ehrling, F. Schwotzer, I. Senkovska, S. Kaskel, and A. Pöppl, J. Phys. Chem. C **126**, 625 (2022).

[12]S. Ehrling, M. Mendt, I. Senkovska, J. D. Evans, V. Bon, P. Petkov, C. Ehrling, F. Walenszus, A. Pöppl, and S. Kaskel, Chemistry of Materials **32**, 5670 (2020).

[13]M. Mendt, F. Gutt, N. Kavoosi, V. Bon, I. Senkovska, S. Kaskel, and A. Pöppl, J. Phys. Chem. C **120**, 14246 (2016).

[14]B. Jee, K. Koch, L. Moschkowitz, D. Himsl, M. Hartman, and A. Pöppl, J. Phys. Chem. Lett. **2**, 357 (2011).

[15]B. Jee, K. Eisinger, F. Gul-E-Noor, M. Bertmer, M. Hartmann, D. Himsl, and A. Pöppl, J. Phys. Chem. C **114**, 16630 (2010).

[16]A. Kultaeva, W. Böhlmann, M. Hartmann, T. Biktagirov, and A. Pöppl, J. Phys. Chem. Lett. **10**, 7657 (2019).

[17]B. Garai, V. Bon, S. Krause, F. Schwotzer, M. Gerlach, I. Senkovska, and S. Kaskel, Chemistry of Materials **32**, 889 (2020).

[18]E. Wasserman, L. C. Snyder, and W. A. Yager, The Journal of Chemical Physics **41**, 1763 (1964).

[19]A. Bencini and D. Gatteschi, *Electron Paramagnetic Resonance of Exchange Coupled Systems* (Springer International Publishing, Cham, 2020).

[20]J. W. H. Schreurs, The Journal of Chemical Physics **69**, 2151 (1978).